SENSITIVITY MEASUREMENTS OF A PASSIVE INTERMODULATION NEAR-FIELD SCANNER

Sami Hienonen, Pertti Vainikainen, and Antti V. Räisänen
Radio Laboratory/SMARAD, Helsinki University of Technology
P.O.Box 3000, FIN-02015 HUT, Finland
E-mail: Sami.Hienonen@hut.fi

Abstract

A passive intermodulation (PIM) near-field XY-scanner for the GSM900 frequency band has been constructed to localize distortion sources in antennas and in other open structures. The equipment should be able to measure distortion levels down to −115 dBm with an input power of 2x20W, since the noise floor of a GSM900 base station is typically around −110 dBm. The sensitivity is limited either by thermal noise or by residual intermodulation distortion depending on the probe coupling. Various causes of residual intermodulation distortion in the PIM near-field measurement are considered and evaluated. Sensitivity measurements of the scanner have been carried out on two test devices. Sensitivities of −112 dBm and −110 dBm have been achieved with an electric and a magnetic field probe, respectively.

Keywords: antenna measurements, near-field scanners, passive intermodulation, sensitivity

1 Introduction

Passive intermodulation (PIM) distortion is a challenging problem in wireless communication systems. It can degrade the system performance whenever multiple signals at different frequencies are transmitted simultaneously. In a GSM900 outdoor base station the transmit power of a channel is typically 43 dBm and the receiver noise floor lower than −110 dBm. This means that the individual components in the antenna path must have sigificantly lower distortion levels. One of the most critical parts is the antenna.

Passive intermodulation level of a device can be measured with dedicated analyzers, but they do not give information on the locations of the distortion sources. By following general guidelines [1, 2], or by experience, one can try to recognize the likely distortion sources. Verifying these assumptions is often very time consuming. For the PIM source localization, a near-field measurement method has been studied previously and PIM levels of −90 dBm have been measured at the GSM900 frequency band with P_{Tx} = 2x43 dBm [3]. In order to extend the usability of the scanner, the sensitivity should be as low as −115 dBm. The sensitivity of the scanner is defined here to be the smallest detectable intermodulation signal power at the device/antenna under test (DUT/AUT).

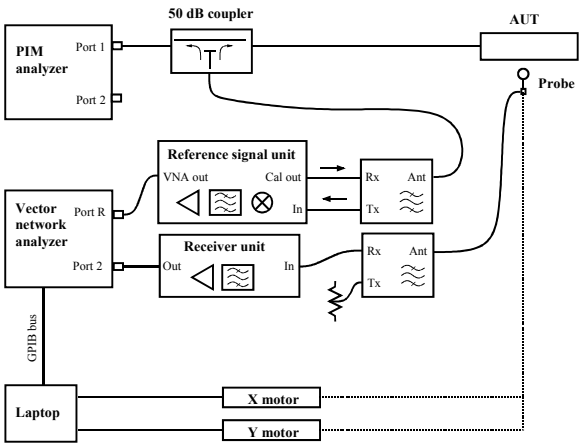

Figure 1. Block diagram of the PIM near-field measurement equipment.

2 PIM scanner

The idea behind the PIM scanner is that a PIM source in an AUT will cause a discontinuity in the reactive near field. This field is scanned with a probe typically at a distance smaller than one tenth of a wavelength like in a common near-field measurement [4]. In the PIM scanner, however, two high power Tx signals are fed to the AUT and the PIM signal is recorded. The scanner is capable of measuring the PIM signal phase as well, which lowers the measurement noise floor and is also useful in the PIM source localization.

It is convenient to compare the scanning results with the reverse PIM level of the AUT. Therefore, the near-field data P_{IM} is normalized with a calibration signal measurement P_{cal}. Knowing the calibration signal level $P_{\mathrm{cal,\ AUT}}$, the PIM level normalized to the AUT is

$$P_{\mathrm{IM,\ AUT}}(x,y) = P_{\mathrm{IM}}(x,y) - P_{\mathrm{cal}}(x,y) + P_{\mathrm{cal,\ AUT}} \quad (1)$$

Knowing the receiver gain G_{rec}, the probe coupling from the AUT can be calculated from

$$C_{\mathrm{probe}}(x,y) = G_{\mathrm{rec}} - P_{\mathrm{cal}}(x,y) + P_{\mathrm{cal,\ AUT}} \quad (2)$$

The block diagram of the PIM scanner equipment is shown in Figure 1. The PIM analyzer is used as a Tx signal source as well as a signal monitor. It is used to check the reverse PIM level of the AUT and the calibration signal level. The reference signal unit generates the reference signal to the vector network analyzer and the calibration signal to the AUT. The measurement is carried out so that the Tx signals are constantly on whereas the calibration signal is alternately on and off making it possible to record P_{IM} and P_{cal} during one scan. The calibration signal level, naturally, must be considerably higher than the measured PIM signal. The probe picks up the calibration and the PIM signals, which are amplified, filtered and finally detected by the Vector Network Analyzer (VNA). The reference signal unit, VNA and the stepping motors are controlled by a computer. The linear guides, AUT/DUT, the probe and the receiver front end are located inside a small shielded anechoic chamber, as seen in Figure 2.

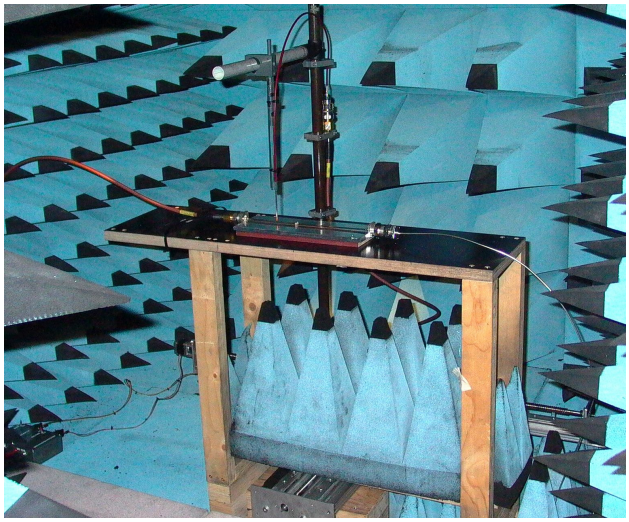

Figure 2. Setup of the PIM near-field scanner sensitivity measurement. An electric field probe scans along a microstrip line.

Two example measurements are shown in Figures 3 and 4. The first one is an x-cut from the sensitivity measurement in Chapter 3.4. A patch antenna and its surroundings were scanned with a magnetic field probe. The normalized PIM level is relatively constant at −120 dBm over the antenna patch area (−62mm < x < 62 mm), whereas it raises to −110 dBm further away from the antenna. The antenna contained no PIM sources in the patch area. In the other example a microstrip line including a PIM source was scanned with an electric field probe, Figure 2. The strip consisted of two tin-copper sheets that were connected together with nylon screws. The ground plane was continuous. Thus, the PIM signal was generated in the poor mechanical contact between the strips. The measured PIM phase and the normalized PIM amplitude are shown in Figure 4. The PIM source is seen as a dip in the amplitude at x = 160 mm. The normalized PIM level of −102 dBm on the left side of the PIM source agrees well with the reverse PIM level −101 dBm of the microstrip. The significance of the phase data is also seen in the graph, since the gradient of the phase points towards the origin of the PIM signal. Thus, in a transmission line, the PIM source does not have to be included in the scanning region; it is sufficient to scan both sides of the source. Because the PIM source is in series with the microstrip, the left and right traveling PIM signals are out-of-phase. This is seen as a jump in the phase and a sharp minimum in the amplitude at the source.

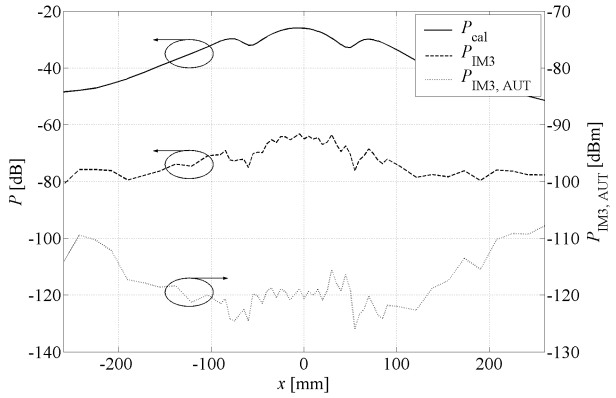

Figure 3. H_y-field scan along a patch antenna and its surroundings. The normalized PIM level $P_{IM3,AUT}$ is calculated according to (1). P_{Tx} = 2x43 dBm, f_{IM3} = 910 MHz, reverse PIM < –120 dBm.

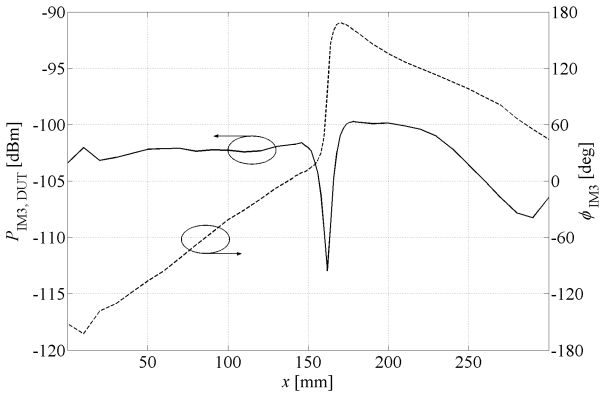

Figure 4. E_z-field scan along a microstrip line with a PIM source at x = 160 mm. PIM phase and normalized PIM amplitude. P_{Tx} = 2x43 dBm, f_{IM3} = 910 MHz, reverse PIM = –101 dBm.

2.2 Near-field probes

The most critical part in the PIM near-field measurement is the near-field probe. Although the power level entering the probe is, at most, on the order of 23 dBm, the field strength is high enough to generate PIM distortion in the probe. Thus, the probes must be designed and constructed very carefully. A number of probes have been designed and tested during the development of the PIM scanner.

The best results have been achieved when the probes were realized with flexible semi-rigid cable, e.g. Sucoform 141, which can be soldered to an N or 7/16-type connector. The magnetic field probe is made of a bended cable to form a short-circuited loop with a narrow gap in the outer conductor. An extended inner conductor of the cable acts as the electric-field probe. The rounded copper stub collects E-field power from wider range and lowers the E-field peak value at the probe, which improves the probe coupling and its PIM performance. Photograph of the magnetic- and electric-field probes is shown in Figure 5.

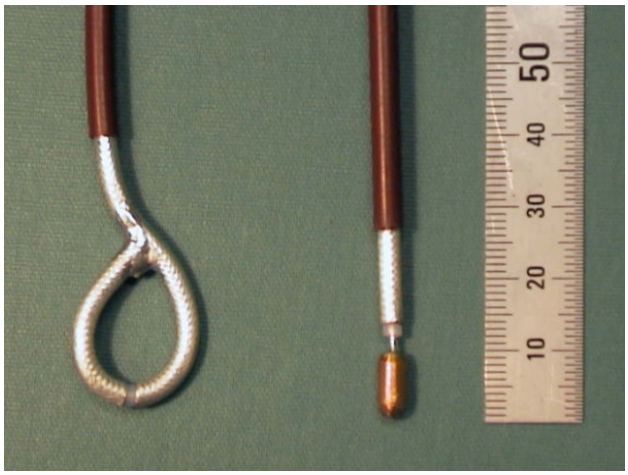

Figure 5. Magnetic and electric field probes.

2.2 Residual intermodulation

Certain guidelines have to be taken care of when performing PIM measurements of antennas [5]. Because the antenna radiates RF energy, the surrounding objects may create a significant amount of PIM distortion. The scanner is problematic in this sense because the moving linear guides cannot be covered with absorbers. However, since the base station antennas usually radiate to the half space they can be pointed towards the ceiling whereas the linear guides lie near the floor. In order to reduce the effect of back radiation, a pyramidal absorber was placed under the table, Figure 2. The chamber without the scanner was tested by measuring a known low-PIM antenna (P_{IM3} < −120 dBm). The antenna was moved on the table with no observable change in the reverse PIM level.

The residual intermodulation distortion detected by the scanner can have a number of causes that may be internal or external to the scanner. The internal distortion sources are inside the receiver, Figure 6, whereas the external sources are located in the environment of the AUT. The possible internal sources are

- probe
- probe cable
- duplex filter
- amplifier–filter chain

and the possible external sources are

- anechoic chamber
- linear guides and stepping motors
- other metallic objects: receiver front end, cables

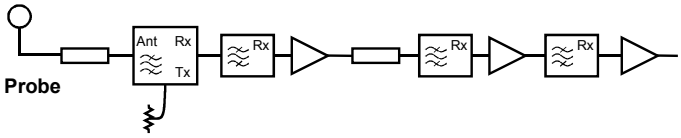

Figure 6. Receiver of the PIM near-field scanner.

3 Sensitivity measurements

The sensitivity of the scanner is limited either by thermal noise or by residual IM distortion of the scanner. The coupling from the AUT to the probe determines which one is the limiting factor of the measurement. When the probe is near the AUT, the coupling and the measured IM signal are high, but then also the coupled Tx power is high possibly resulting in residual IM distortion in the receiver. Instead, if the probe is moved further away from the AUT, the residual IM level decreases more than the measured signal but then noise starts to limit the measurement. However, external PIM sources may create background intermodulation distortion that does not depend on the probe coupling.

3.1 Test devices

The performance of the scanner was tested by scanning a low-PIM microstrip line and an antenna. The aim was to separate the internal and external distortion sources with the non-radiating and radiating test devices. Additionally, the receiver without the probe was tested by a conventional IM measurement.

The microstrip line was constructed from a tin-copper sheet with Rohacell foam as a substrate. 7/16-connectors were attached to the aluminum ground plane. The reverse PIM level was below −120 dBm, f_{IM3} = 890…915 MHz, P_{Tx} = 2x43 dBm.

The test antenna was a stacked patch antenna with a silver plated ground plane and an N-connector. The reverse PIM level of the antenna was below −118 dBm, f_{IM3} = 890…915 MHz, P_{Tx} = 2x43 dBm.

3.1 Thermal noise and cable leakage

The noise behavior of the scanner is governed by the receiver front end; specifically by the losses of the probe, probe cable and filters, and by the LNA noise figure. The noise level was measured with the probe connected to the receiver. The input reduced noise density was −172±1 dBm/Hz.

Cross talk between the transmitter and the receiver may cause a bias signal in a near-field measurement [6]. The transmitter and the receiver cable leakages were evalu-

ated by terminating the cables in turn. The measured signal was at the noise floor.

3.2 Probe cable

The probe cable should have low loss, low PIM distortion level, and it should be flexible in order to allow scanning. An RG 393 cable was chosen for this purpose. It has a length of 2.5 m, an attenuation of 0.7 dB and a PIM level below −120 dBm, f_{IM3} = 910 MHz.

3.3 Receiver

The receiver (without the probe) was tested by applying Tx signals directly to the duplex filter antenna port. The input reduced PIM distortion level was −153 dBm (P_{Tx} = 2x23 dBm) with the PIM level dependency on the Tx level of 2.1 dB/dB. This will not limit the performance of the scanner since the level corresponds to $P_{IM3,\,AUT}$ = −133 dBm with a probe coupling of 20 dB.

It should be noted that the duplex filter is essential in the receiver front end and that its Tx port must be matched. Otherwise, the PIM sources in the probe and the cable would see a reactive load and there would be standing waves at the Tx frequencies. This would lead to an unpredictable distortion level.

3.4 Near-field probes

In all the scans P_{IM3} was measured with P_{Tx} = 2x43 dBm, f_1 = 935 MHz and f_2 = 960 MHz. Intermodulation frequency was 910 MHz. Probe height from the DUT/AUT surface was 10 mm.

In the first measurement, the microstrip line was scanned with an electric-field probe. The normalized PIM level was below −113 dBm in the strip area. In the second measurement, the test antenna and its surroundings were scanned. The normalized PIM level remained mostly below −117 dBm, as seen in Figure 7. However, along the line x = 0 mm, where E_z-field has a deep minimum, the normalized level raises up to −101 dBm. It turned out that near the antenna center P_{IM3} is relatively constant along the x-direction whereas P_{cal} has the minimum. This suggests that the detected PIM originates in the probe caused by the horizontal field components. The same phenomenon could explain the raised PIM levels at x = ±100 mm. In addition, some background PIM is seen further away from the antenna region. This is probably caused by the external PIM sources.

In the magnetic field scan the residual PIM level remained below −115 dBm in the patch area, Figure 8. Contrary to the E-field measurement, the normalized PIM is typically lower near the edges than over the patch. This can be seen in the x-cut of the data, Figure 3 . In addition to background PIM, thermal noise limits the sensitivity at the edges of the scanning area.

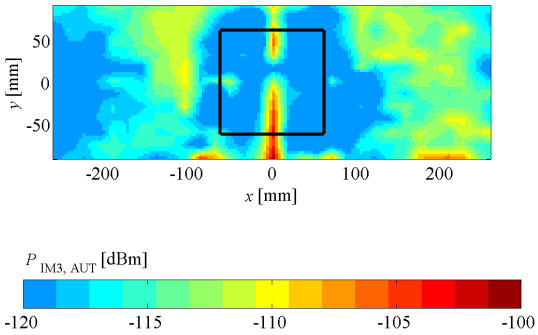

Figure 7. E_z-field scan along the test antenna, normalized PIM level. Outline of the patch is drawn with a black line. P_{Tx} = 2x43 dBm, f_{IM3} = 910 MHz.

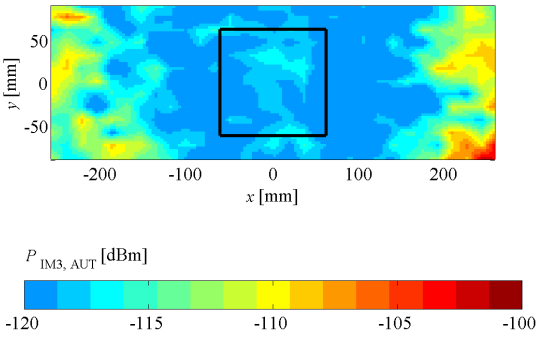

Figure 8. H_y-field scan along the test antenna, normalized PIM level. Outline of the patch is drawn with a black line. P_{Tx} = 2x43 dBm, f_{IM3} = 910 MHz.

3.5 Edge effect

As mentioned earlier, the normalized PIM level tends to increase or decrease when the probe is the near metal edges of the AUT. An example of this phenomenon is shown in Figure 9, where the E_z-field across a microstrip line is recorded. The PIM signal reaches its minimum at a different location than the calibration signal. As a result, the normalized PIM level peaks at this minimum while being essentially constant over the strip. It could be that the E_y-field, which has a maximum near the E_z-minimum, couples to the probe and causes the increase in $P_{IM3,\,DUT}$. A different probe was used in here as in the sensitivity measurements. In general, the edge effect is not so clear and the location and the level of the PIM distortion near metal edges vary. This behavior is typical for a PIM source, which usually needs considerable amount of time to settle down [7].

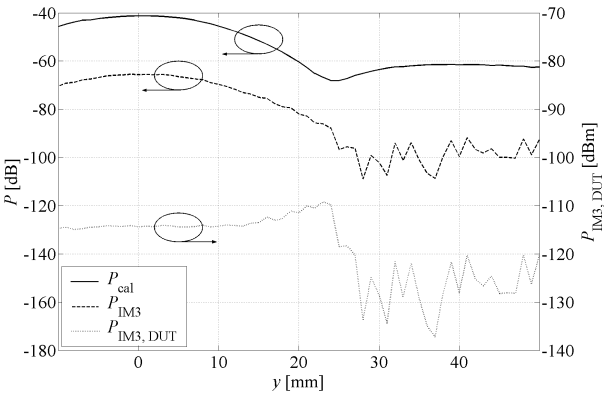

Figure 9. Edge effect. E_z-field scan across a microstrip line. The strip extends from −7.5 to 7.5 mm.

4 Discussion

The external distortion sources do not seem to limit the scanner performance because also the microstrip line measurements showed raised PIM levels near the strip edges. There was probably some background PIM in the antenna measurements but it did not dominate near the patch area. Furthermore, the probe cable, connector and the receiver are performing well since the recorded PIM level is independent of the probe coupling. Thus, the main limitation of the scanner is the PIM performance of the probe. Between different probes there are clear variations in the residual PIM level caused by the edge effect. Thus, the effect can be minimized by a careful probe design and construction.

It should also be noted that the reverse PIM level was not affected by the scanning although the probe height from the AUT was only 10 mm.

Based on the results presented in this paper an estimation of the scanner sensitivity is shown in Table 1. The sensitivity depends on the coupling from the AUT to the probe and is either thermal noise or residual PIM limited. The table does not take into account the edge effect that degrades the sensitivity near metal edges. In order to minimize the edge effect and to preserve the dynamic range of the measurement, the coupling should be around 30–40 dB.

Table 1. Estimated sensitivity of the scanner. *SNR* = *SIR* = 5 dB. P_{Tx} = 2x43 dBm, f_{IM3} = 910 MHz.

Probe coupling [dB]	Sensitivity [dBm]		
	Limited by noise	Limited by system IM	
		E-field	H-field
20	−141	−112	−110
40	−121		
60	−101		

5 Conclusions

The sensitivity of the passive intermodulation near-field scanner has been tested by scanning low-PIM test devices. The residual intermodulation level was mainly below −117 dBm and −115 dBm for the electric and magnetic field probes, respectively. It was found that the near-field probe is the most critical part in the PIM scanner, which is relatively straightforward to implement into existing PIM equipment. Although there were raised intermodulation power levels at the edges of the antenna., the sensitivity of the near-field measurement equipment seems to have sufficient fidelity for many GSM900 base station antennas.

6 Acknowledgements

This work has been partially funded by the Academy of Finland.

7 References

[1] P. L. Lui and A. D. Rawlins, Passive non-linearities in antenna systems, *IEE Colloquium on Passive Intermodulation Products in Antennas and Related Structures, Digest No. 1989/94*, London, Jun 7, 1989, pp. 6/1–6/7.

[2] B. G. M. Helme, Interference in telecomm systems, from passive intermodulation product generation: an overview, *Proceedings of the 22nd Antenna Measurement Techniques Association Annual Symposium (AMTA 2000)*, Philadelphia, Oct 16–20, 2000, pp. 143–149.

[3] S. Hienonen, V. Golikov, V. S. Möttönen, P. Vainikainen and A. V. Räisänen, Near-field amplitude measurement of passive intermodulation in antennas, *Proceedings of the 31st European Microwave Conference EuMC 2001, Vol. 2*, London, Sep 25–27, 2001, pp. 277–280.

[4] J. S. Dahele and A. L. Cullen, Electric probe measurements on microstrip, *IEEE Trans. Microwave Theory Tech.*, vol. 28, Jul 1980, pp. 752–755.

[5] Y. Patenaude, C. K. Mok, Some recommendations about the PIM measurement of antennas, *Proceedings of the 22nd Antenna Measurement Techniques Association Annual Symposium (AMTA 2000)*, Philadelphia, Oct 16–20, 2000, pp. 155–159.

[6] A. C. Newell, Methods to estimate and reduce leakage bias errors in planar near-field antenna measurements, *Proceedings of the 24th Antenna Measurement Techniques Association Annual Symposium (AMTA 2002)*, Cleveland, Nov 3–8, 2002, pp. 60–64.

[7] Y. Patenaude, J. Dallaire, F. Ménard, S. Richard, Antenna PIM measurements and associated test facilities, *Proceedings of the IEEE Antennas and Propagation Society International Symposium 2001, Vol.4*, Boston, Jul 8–13, 2001, pp. 620–623.